STRATEGIC EVACUATION FOR REGIONAL EVENTS: WITH AND WITHOUT AUTONOMOUS VEHICLES

Jooyong Lee
Department of Civil, Architectural and Environmental Engineering
The University of Texas at Austin
jylee3302@utexas.edu

Kara M. Kockelman, Ph.D., P.E.
(Corresponding Author)
Dewitt Greer Centennial Professor of Transportation Engineering
Department of Civil, Architectural and Environmental Engineering
The University of Texas at Austin – 6.9 E. Cockrell Jr. Hall
Austin, TX 78712-1076
kkockelm@mail.utexas.edu

Word Count: 5,231 words + 4 tables × 250 = 6,231 words

Transportation Research Record 2675(9): 1398-1409, 2021

Submitted July 30, 2020

ABSTRACT

An evacuation scheduling algorithm is developed for optimal planning of large-scale, complex settings to minimize total delay plus time in transit across residents. The algorithm is applied to the 8-county Houston-Galveston region and land use setting under the 2017 Hurricane Harvey scenario, with multiple shelters as destinations, far from the Gulf of Mexico. Autonomous vehicle (AV) use under central guidance is also tested, to demonstrate the evacuation time benefits of AVs. Having a higher share of AVs delivers more efficient evacuation performance, due to greater reliability on routes selected, lower headways, and higher road capacity. 100% AV use delivers lower overall evacuation costs and network clearance times (from 89 hr. to 68 hr. network clearance time, assuming 1.88 vehicles per household) and lower uncertainty in travel times (from reduced standard deviation of 12 hr. to 9 hr.). Other scenarios were also tested. For example, a 3% to 5% compressed network clearance time added 10% to 25% longer travel times and network congestion. A 6% longer network clearance time reduced residents' total travel time and network congestion by 10%, but increased the evacuation cost, demonstrating the benefits of scheduling (and enforcing) evacuations across residents and neighborhoods more thoughtfully. Optimal combination of departure times by neighborhood and household helps balance these conflicting objectives.

KEYWORDS

Evacuation; Hurricane; Departure Time Scheduling; Fleet Management; Autonomous Vehicles

BACKGROUND

Disasters like hurricanes, wildfires, flooding, and hazardous material releases are major threats to life and property in populated settings. Well-timed and directed evacuation is a key response to impending or live disasters, but the complexity of large metropolitan areas makes such a response quite challenging. To tackle this question, different evacuation strategies for different types of natural disasters (Takabatake et al., 2017; Takagi et al., 2016), contraflow operations on network links (Pyakurel et al., 2017) and strategic sheltering (Liu & Lim, 2016) have been studied. This paper emphasizes departure time scheduling and use of autonomous vehicles (AVs) before and during hurricanes.

Heavy winds and rainfall tend to follow a hurricane's trajectory, affecting the location and time of flooded streets and highways. Smart destination choices, departure time choices, and route choices can make the difference between life and death, as well as comfortable versus overly congested, stressful and/or dangerous travel to safe zones. In the future, communities may also be able to call on fleets of shared AVs to rescue their most vulnerable populations and/or ensure that evacuation is orderly. Centrally controlled AVs can be directed in real time, with recourse in routing, which is helpful. With faster driving-response times, AVs may also deliver shorter headways and higher capacity flow that proves very valuable during evacuations. Having large shares of AVs in our traffic streams is a long way off, due to technology, cost, adoption rates, and regulatory challenges, so this paper focuses primarily on conventional-vehicle evacuations.

Evacuee behaviors and willingness to depart (as well as route and destination choices) are impacted by social bonds with others, including strength of tie (family, friend, pet, or colleague, for example), contact frequency (daily or monthly), and geographical proximity (Sadri et al., 2017). Cell phone communications, Internet sites, and smartphone apps are also now common for social interaction during evacuations. For example, Twitter response reached its peak during the pre-impact and preparedness phase of Florida's Hurricane Matthew landfall in 2016 (Martín et al., 2017). Interactions also include public agency information and official warnings. Once a mandatory evacuation is ordered, the response to the warning messages can vary among population groups (Huang et al., 2016; Morss et al., 2016) and result in different outcomes. In the case of inconsistent evacuation orders, the public can misinterpret the severity of the hazards and refuse to leave (Elder et al., 2007). Thus, evacuation orders must be carefully designed to elicit coordinate, effective and timely responses of households and businesses in the affected areas.

A generally held belief is that the evacuees should avoid the threat as soon as possible. This results in heavy early evacuation demands, which are likely to fall over hours or days, forming an S-shaped curve (Li et al., 2013). Many evacuation experts find that designing strategic delays in departure times delivers faster evacuation overall, by avoiding unnecessary congestion delays (Lämmel & Klüpfel, 2012; Madireddy et al., 2015). Asking and/or forcing subsets of evacuees in low-risk areas to delay their departures can improve performance dramatically (Madireddy et al., 2015). Metering of evacuation flows and/or implementing phased evacuation strategies are also possible interventions or controls (Lämmel & Klüpfel, 2012). However, multi-stage evacuations should be carefully designed, since too many stages can cause lower discharge rates and longer total evacuation than desired (Chien & Korikanthimath, 2007).

Key variables are the departure time schedule, total evacuation time span, arrival times at shelters, and total time spent en route by evacuees. The departure time schedule is the distribution of individual evacuees' departure times over time, as embodied in the slope or flow rate of the S-shaped departure curve. The evacuation time span defines how long the evacuation order should last; it is the time duration of the region's S-shaped departure curve. If the evacuation time span is too short, internal gridlock effects can cause excessive delays and some drivers may be unable to evacuate the network in due time (Tamminga et al., 2011). Therefore, an efficient evacuation plan should consider both the departure time of each individual evacuee according to individual's condition, and the total time span for all evacuees to depart the endangered area or zones. This can be structured as a bi-level optimization problem, where a local government issues temporal evacuation orders, and the citizens in a network evacuate considering the risk, traffic conditions, and infrastructure (Abdelgawad et al., 2010; Apivatanagul et al., 2012).

METHODOLOGY

One can view the evacuation problem as a type of bi-level game, with a strategic leader (e.g., local government) making evacuation orders first (upper level) and evacuees moving sequentially in space (lower level). The leader can update the strategy dynamically, as desired (e.g., in response to local flooding of streets or higher than expected demand or lower than expected capacity on certain links). This paper assumes that the leader orders evacuation timing for all evacuees' vehicles with the objective to minimize the average evacuation cost per vehicle needed to finish the evacuation, recognizing that evacuees will decide their destinations and routes. Here, evacuees have access to real-time travel times and can re-route every 5 minutes. This work uses the Simulation of Urban Mobility (SUMO) code (Lopez et al., 2018), along with bi-level optimization, reflecting interactions between the leader and evacuees.

Evacuation Orders (Upper Level)

In the upper level optimization, the departure time schedule, p (where p is the set of p_γ and p_γ is the portion of vehicles departing in the discrete time interval γ defined in Eq. (1)), and the evacuation time span, T (e.g., 24 hours), are adjusted sequentially to seek an optimal strategy. Discrete vehicles depart according to a Poisson random number generator within each time interval. Late arrivals at shelters is not desirable for most evacuees, since long travel times are undesirable for most evacuees. Nonetheless, many evacuees will prefer having sufficient time before departing from their homes to pack more items and better prepare for their life away from home. When every evacuee decides to evacuate as soon as possible (e.g., p_1 = 1.0), shelter arrival times may be relatively early, but travel times will be long for most due to excessive network congestion. The travel time can be shorter when the evacuation order is made uniformly to maintain low network congestion (e.g. $p_\gamma = 0.2, \forall\gamma \in [1,5]$), but, in this case, some evacuees may evacuate too late or the network clearance time can be unnecessarily long. Also, it is not guaranteed that uniformly distributed departure time schedules will result in optimum evacuation cost.

$$p = (p_1,\ p_2,\ p_3,\ p_4,\ p_5) \tag{1}$$

$$s.t.\ \ \mathrm{T} \in [0,24] \text{ in hours}, \sum_{t=1}^{5} \mu_t = 1$$

Even though the departure time schedule is designed optimal across the evacuation time span, T, the network congestion can be excessive if T is not large enough. On the other hand, with an excessively large evacuation time span, some evacuees may evacuate too late resulting in low evacuation performance. Therefore, the optimal combination of p and T is needed to maximize the evacuation performance. The objective of the upper level optimization is to minimize the average evacuation cost per evacuee with the two decision variables, departure time schedule (p) and evacuation time span (T). The evacuation cost is determined by the sum of travel time and the difference between departure time and the disaster onset time. Excessive travel time will adversely affect the evacuation performance by increasing the uncertainties from the traffic congestion and possible threats on the roads during the evacuation. Unnecessarily early departure may cause the evacuees to not have enough time to prepare their evacuation, while considerably late departure may threaten their evacuation.

Upper-level optimization is achieved by a genetic algorithm using real numbers. A genetic algorithm is useful for the minimization of average evacuation cost because it avoids being trapped in a local optimal solution, and its structure facilitates parallel computing to effectively search the solution. A summary of the upper level optimization is shown in Eq. (2).

$$C_{vijt} = \Psi_{vijt} + \left|\Phi_i - \Delta_{vij}\right| \tag{2}$$

$$\underset{p,T}{arg\ min} \sum_{v \in V} \sum_{i \in I} \sum_{j \in J} \sum_{t \in T} \frac{C_{vijt}}{n}$$

V: Set of evacuating vehicles; $v \in V$

I: Set of origins; $i \in I$

J: Set of destinations (pre-defined by the local government); $j \in J$

T: Evacuation time span, where $t = 1,2,3 \dots, T$

Ψ_{vijt}: Travel time of vehicle v departing from i to j at time t, subject to lower level problem

Φ_i: The time when the disaster began i, subject to lower level problem

Δ_{vij}: The departure time of vehicle v departing from i to j, subject to lower level problem

C_{vijt}: The Evacuation cost of vehicle v departing from i to j at time t

n: Number of evacuating vehicles

Transportation Simulation (Lower Level)

In the lower level optimization, discrete vehicles depart according to the evacuation order from a Poisson random number generator within each time interval p_γ until time T. After every vehicle has arrived at the destination, the average evacuation cost will be estimated to evaluate the evacuation performance of the given p and T combination.

SUMO, with a Python API named TraCI for customization, is used for simulating transportation during evacuation. SUMO's mesoscopic simulation option is implemented, since a coarser model for vehicle movements had an advantage in simulation time over detailed microscopic models in a large-scale network. In this setting, each link is divided into homogenous cells, and the flow across the cells is determined by a function of traffic density threshold. An A-Star (A*) algorithm is used to find the shortest path, and a one-shot assignment of re-routing each vehicle in every 5 minutes is applied. Two different vehicle classes, human-driven vehicle (HV) and autonomous vehicle (AV) are simulated. AVs' short reaction time and communication capability may allow increased road capacity obtained from smaller spacing between vehicles. The road capacity (q_{max}) with respect to the vehicle penetration rate (R_m) is calculated with Eq. (3) obtained from (Levin & Boyles, 2016), and converted it to the time headway (3600/q_{max} second) needed for mesoscopic simulation. Assuming a free flow speed (u_f) of 60 mi/h, vehicle length (l) of 20 ft., HV's reaction time (Γ_{HV}) 1 s, and AV's reaction time (Γ_{AV}) 0.5 s, the headway between vehicles is 1.23 s (AV 0%), 0.98 s (AV 50%), and 0.73 s (AV 100%) in each AV market penetration scenario.

$$q_{max} = u_f \frac{1}{u_f \sum_{m \in \{AV,HV\}} R_m \Gamma_m + l} \tag{3}$$

The destination of each vehicle is determined by the negative exponential of volume-to-capacity ratio ($exp\,(-V_j/C_j)$) of the shelter j from the shelter set J. Before a vehicle decides to leave the origin, the performance of every shelter j will be estimated, and the probability to select a certain shelter j will be estimated ($Pr(j)$) according to the shelter's performance. The destination choice will be made by following this shelter probability distribution shown in Eq. (4).

$$Pr(j) = \frac{exp\,(-V_j/C_j)}{\sum_{s \in J} exp\,(-V_s/C_s)} \tag{4}$$

A disaster simulation is performed with the transportation simulation, so that certain links will be under risk from the natural disaster. The evacuation demand is assumed to be proportional to the risk level of the origin, and a link is closed according to the risk level within its traffic analysis zone (TAZ). If a link is closed, this link will be penalized to have a travel time close to infinity to prevent it from being used during the route search process. Therefore, the transportation network in this model is changing over time (time-varying network) depending on the disaster scenario.

Model Summary

The evacuation simulation is posed as a bi-level optimization. The upper level problem determines the evacuation order of departure time schedule and evacuation time span. The departure time schedule refers to the temporal distribution of evacuation demand, and the evacuation time span is the length of time needed for all evacuees to depart from their origins. The lower level problem simulates the natural disaster, route choice, and traffic congestion according to the evacuation order. Discrete vehicles will be departing under the evacuation order from a Poisson random number generator within each time interval p_γ until time T. Disaster simulation affects the evacuation demand and the network infrastructure. The objective of the simulation is to minimize the average evacuation cost, and a genetic algorithm is used for the optimization. Figure 1 shows the flowchart of the proposed evacuation simulation.

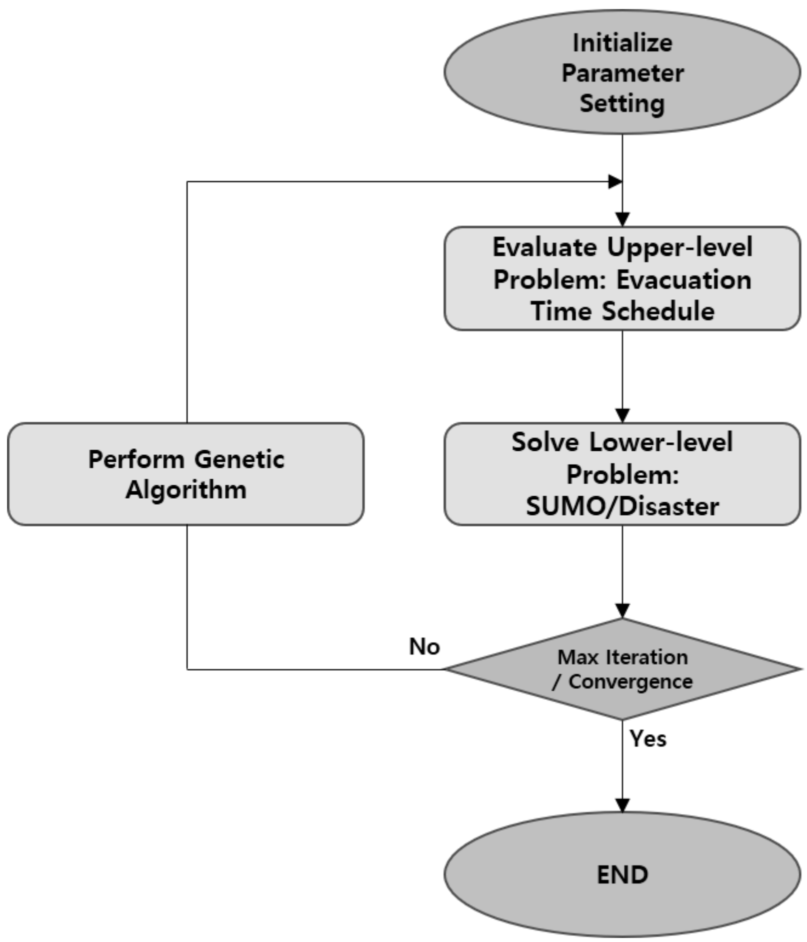

Figure 1. Evacuation Simulation Flowchart

EVACUATION SIMULATION

The developed evacuation model can be used for any transportation network and any type of disaster (e.g., firestorm, nuclear meltdown, terrorist attack, tsunamis, and volcanic activities) if the network configuration and disaster data are provided. This paper simulates evacuation from a flood in Houston, TX to evaluate the model performance.

Flood Modeling

In 2017, Hurricane Harvey touched down on the Texas Gulf Coast, US, and caused $125 billion in damages. These damages were the most extensive of any natural disaster in US history, other than Hurricane Katrina. Nearly one third of Houston was flooded, and 40,000 people had to evacuate to shelters (Blake & Zelinsky, 2018). Houston Metropolitan Area with 8 counties (Brazoria, Chambers, Fort Bent, Galveston, Harris, Liberty, Montgomery, and Waller) is simulated in this paper.

The flood modeling requires the data of time, location, and depth of flooding. The simulation date is Aug. 27, 2017, with the flood data from the United States Geological Survey – National Water Information System (USGS-NWIS) (USGS, 2020), and Federal Emergency Management Administration (FEMA) (FEMA, 2018). Aug. 27 was chosen for the evacuation scenario because the flooding started around this date and lasted until early September. USGS-NWIS provides the gage height of US surface-water sites (rivers and creeks) over time, so that the exact time of flooding can be identified. FEMA provides the flood depth map to estimate an individual link's risk level.

In this paper, when a surface-water site from USGS-NWIS is identified as flooded, the site's nearby traffic analysis zones (TAZs) are also assumed to be flooded. When a TAZ is flooded, every link in this TAZ is also assumed to be flooded. The initial USGS-NWIS data show 37 sites were flooded from Aug. 26 to Aug. 28, 2017, and an additional 3 sites near the coastline were assumed to be flooded from the beginning of the simulation due to the storm surge. Although the time and location of flooded links can be identified from the USGS-NWIS data, the severity of the disaster and the flood depth should be obtained from FEMA's Harvey Flood Depth Grid data. FEMA provides a gridded flood depth map of Hurricane Harvey, and only the study area of 8 counties is used in this paper. From the gridded flood depth map, a link's flood depth can be determined by its nearest grid's flood depth. Figure 2 and Table 1 shows the details of the flood data.

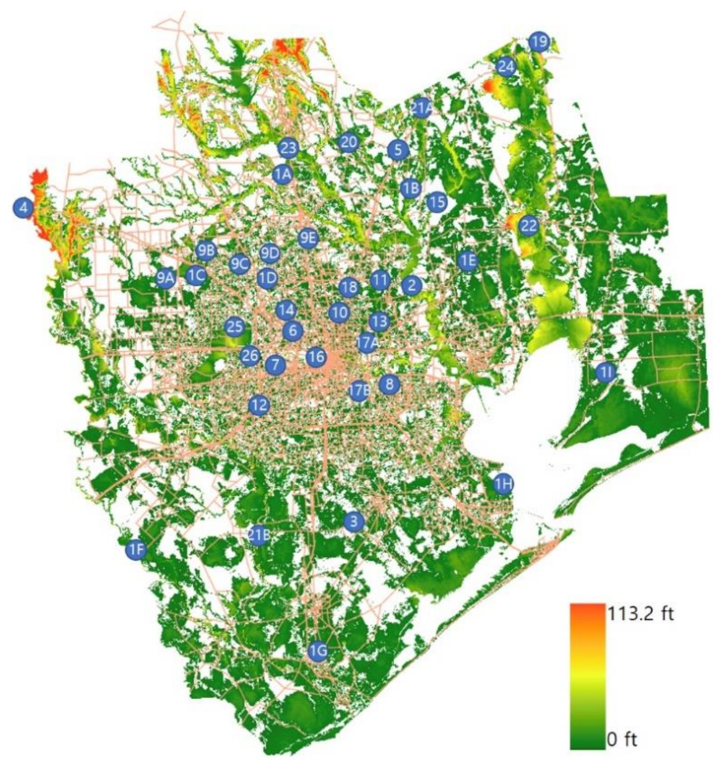

Figure 2. USGS-NWIS Data Points (Blue Dots) and FEMA Flood Data (Contour Map)

Table 1. USGS-NWIS Data and Evacuation Scenario

Site ID	Site Name	Time of Flooding from Data	Scenario
1A	Panther Br at Gosling Rd, The Woodlands	Aug. 26, 11:15	-
1B	E Fk San Jacinto Rv, New Caney		
1C	Cypress Ck at House-Hahl Rd, Cypress		
1D	Greens Bayou at Cutten Rd, Houston		
1E	Cedar Bayou, Crosby		
1F	San Bernard Rv, Boling		
1G	Bastrop Bayou at CR 288, Lake Jackson	Aug. 26, 11:15 (assumed)	
1H	Moses Lk-Galveston Bay, Texas City		
1I	E Fk Double Bayou at Carrington Rd, Anahuac		
2	Lk Houston, Sheldon	Aug. 26, 12:00	
3	Chocolate Bayou, Alvin	Aug. 26, 12:15	
4	Brazos Rv, Hempstead	Aug. 26, 13:30	
5	Peach Ck at Splendora	Aug. 26, 21:00	
6	Brickhouse Gully at Costa Rica St, Houston	Aug. 26, 21:45	
7	Buffalo Bayou at Piney Point	Aug. 26, 22:30	
8	Vince Bayou at Pasadena	Aug. 26, 23:45	
9A	Cypress Ck at Katy-Hockley Rd nr Hockley	Aug. 27, 00:00	All residents in flooded areas must evacuate from Aug. 27, 00:00
9B	Little Cypress Ck, Cypress		
9C	Cypress Ck at Grant Rd, Cypress		
9D	Cypress Ck at Stuebner-Airline Rd, Westfield		
9E	Cypress Ck, Westfield		
10	Halls Bayou at Houston	Aug. 27, 01:00	Evacuate according to flood severity
11	Garners Bayou, Humble	Aug. 27, 01:15	
12	Keegans Bayou at Roark Rd, Houston	Aug. 27, 01:30	
13	Greens Bayou at Ley Rd, Houston	Aug. 27, 02:00	
14	Whiteoak Bayou at Alabonson Rd, Houston	Aug. 27, 03:00	
15	Luce Bayou abv Lk Houston, Huffman	Aug. 27, 03:15	
16	Buffalo Bayou at Houston	Aug. 27, 06:00	
17A	Hunting Bayou at IH 610, Houston	Aug. 27, 06:45	
17B	Sims Bayou at Houston	Aug. 27, 06:45	
18	Greens Bayou, Houston	Aug. 27, 07:00	
19	Menard Ck, Rye	Aug. 27, 11:15	
20	Caney Ck, Splendora	Aug. 27, 12:00	
21A	E Fk San Jacinto Rv nr Cleveland	Aug. 27, 15:45	
21B	Brazos Rv nr Rosharon	Aug. 27, 15:45	
22	Trinity Rv at Liberty	Aug. 27, 19:15	
23	W Fk San Jacinto Rv, Conroe	Aug. 27, 23:30	
24	Trinity Rv at Romayor	Aug. 28, 16:45	Everyone must evacuate at Aug. 28, 00:00
25	Langham Ck nr Addicks	Aug. 30, 07:00	
26	Buffalo Bayou at W Belt Dr, Houston	Aug. 30, 17:30	

The evacuation demand induced from the flood is proportional to the flood depth of its origin link. A link will be closed by the probability derived from the ratio of the link's flood depth and the deepest depth recorded in its TAZ. If a link is closed, a value close to infinity will be assigned for the link's travel time, so that this link will be penalized in the route searching process. Only the vehicles departing from the closed link can leave this link without travel time penalties.

Simulation Setting

The transportation network used in this paper is for the 8-county Houston Metropolitan Area of Texas, with 36,120 links, 18,448 nodes, and 10 shelter locations, as shown in Figure 3. Table 2 shows the number of evacuating passenger vehicles, 4,346,151 vehicles in total, estimated from the population, household size per county, and passenger vehicle ownership statistics (FHA, 2017; Bureau, 2019). Other vehicle types (e.g., heavy-duty trucks, buses, and motorcycles) and public transit services are not included in this paper. The number of vehicles evacuating each TAZ is assumed to be proportional to the daily number of trips originating in that TAZ, with TAZ links randomly selected for the home location of each household.

Table 2. Evacuation Demand Estimation

County	Population (US Census Bureau, 2019)	Persons / Household (US Census Bureau, 2019)	# of Households
Brazoria	37,426	2.88	12,995
Chambers	43,837	2.96	14,810
Fort Bend	811,688	3.18	255,248
Galveston	342,139	2.69	127,189
Harris	4,713,325	2.88	1,636,571
Liberty	88,219	2.85	30,954
Montgomery	607,391	2.86	212,374
Waller	55,246	3.07	17,995
Sum	6,699,271	-	2,308,137

# of Households	Vehicle Ownership per Household (FHA, 2017)	# of Vehicles
2,308,137	1.88	**4,346,151**

In Figure 3, 10 high schools outside of the Texas State Highway Beltway-8 are chosen for shelters. Each shelter *j*'s capacity is assumed to be 10% of the total demand, and evacuees will choose their destination by the shelter's volume-to-capacity ratio. The shelter's volume can exceed the capacity, but it will be penalized by having a high volume-to-capacity ratio as stated in Eq. (3). The parameter settings for genetic algorithm are population size to 10, ranking selection with 60% survival rate, 10% mutation rate and 50 iterations. In the simulation, only 0.1% of the total number of vehicles estimated in Table 2 are used due to the high computational cost. The capacity of roads is reduced proportional to the sampling rate to preserve traffic congestion characteristics.

Figure 3. Transportation Network and Shelter Locations (A to J)

Simulation Results

Figure 4 shows the optimization results of 3 AV scenarios (AV 0%, AV 50%, and AV 100%). The genetic algorithm minimized the evacuation cost, and the evacuation cost after optimization is smaller with more AVs in the simulation. This is considered to be the impact of AVs' improved driving performance that allows for smaller spacing and shorter reaction time. The improvement in driving performance may reduce traffic congestion, thereby lowering travel time. The low traffic congestion in the AV scenario enabled the evacuees to determine their departure time flexibly, which resulted in lower evacuation cost.

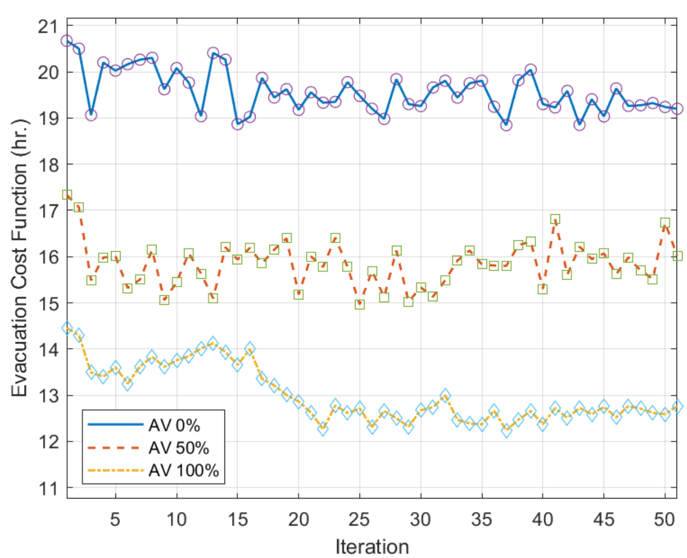

Figure 4. Evacuation Cost Minimization

Table 3 shows the optimization results of departure time schedule (p) and evacuation time span (T). For example, in AV 50% departure time schedule, 45% of the total vehicles depart from t=0 to t=21/5 hr., 20% depart from t=21/5 to t=42/5 hr., and so forth, until the last vehicle departs at the end of evacuation time span (t=21 hr.). The evacuation time span (T) is not sensitive to the AV penetration rate in the network, which represents that it is more subject to the flood timeline. Figure 5 shows the transportation simulations of each AV scenario's optimization results with departure and arrival curves. In Figure 5-(c), the AV 100% scenario, a sharp increase is observed in the early stages of the departure curve, indicating more vehicles can be loaded into the network with AVs.

Table 3. Optimization Results

	AV 0%	AV 50%	AV 100%
Departure Time Schedule (p)	(52%, 8%, 18%, 8%, 14%)	(45%, 20%, 16%, 4%, 15%)	(60%, 13%, 14%, 3%, 10%)
Evacuation Time Span (T)	23.3 hr.	21 hr.	22.2 hr.

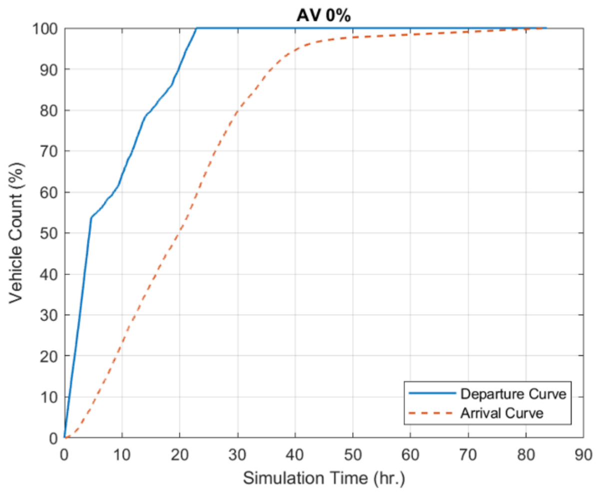

(a)

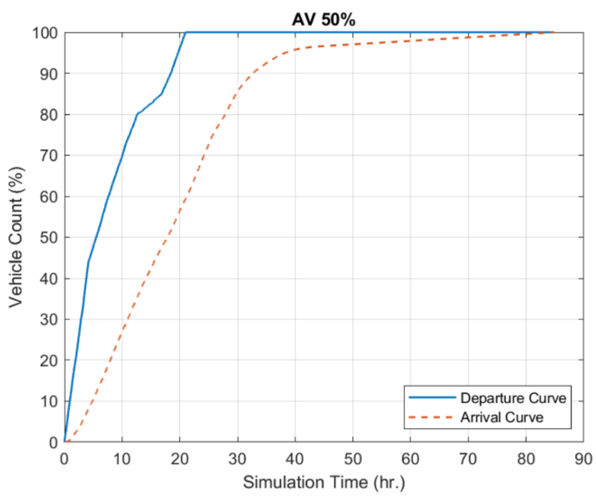

(b)

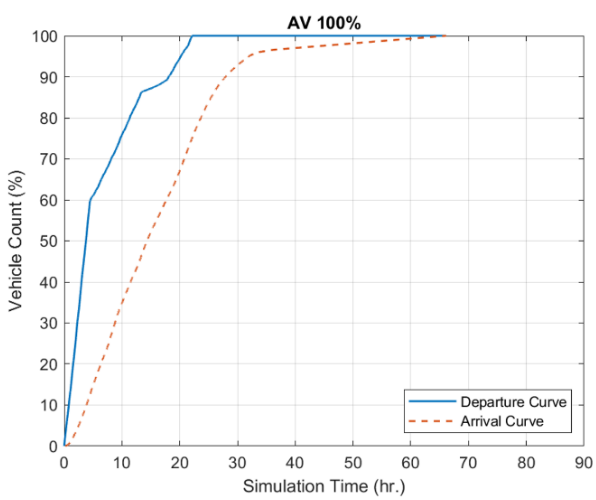

(c)

Figure 5. Departure-Arrival Curve by AV Scenario

Evacuation Performance by AV Scenario

Figure 6 shows the evacuation performance by repeating the transportation simulation 5 times under each scenario's optimization results. In Figure 6-(a), the average evacuation cost per vehicle (hr./veh) decreases with more AVs in the network, where the AV 100% scenario shows a 30% reduction (from 16.8 to 12 hr.) in average evacuation cost compared to the AV 0% scenario. The standard deviation of evacuation cost between evacuees also decreases as there are more AVs in the network. Based on these results, more efficient, safe, and reliable evacuation may be possible with AV adoption.

According to Figure 6-(b), the average and standard deviation of travel time follow the same trend as the evacuation cost estimates. The AV 100% scenario shows around a 30% and 20% reduction of average and standard deviation, respectively, in travel time compared to the AV 0% scenario. With shorter travel times, more evacuees can avoid possible threats until they reach the shelter, and the infrastructure flexibility can be improved to actively respond to the evacuation demand.

Figure 6-(c) quantifies the network congestion by demonstrating congestion as the ratio between the vehicles' travel time and the free-flow time expected when traveling on a route at the speed limit. This value becomes closer to 1 when the vehicle is traveling in free flow, and it increases when the vehicle experiences congestion. As expected from the travel time analysis, increasing the number of AVs results in less congestion.

The network clearance time after simulating each scenario 5 times, as shown in Figure 6-(d), represents the time when the last evacuee arrived at the shelter and no more vehicles are left in the network. The results suggest that it will take 3 to 4 days, even with full AV adoption, to evacuate everyone across the 8-county Houston region. Considering the fact that everyone chose to leave within the first 21 to 23 hours as calculated from the evacuation time span, the total time needed to finish the evacuation takes 3 to 4 times longer due to traffic congestion. Therefore, additional operational methods (e.g., lane reversal, shared vehicles) should be combined with AV adoption to further reduce the clearance time.

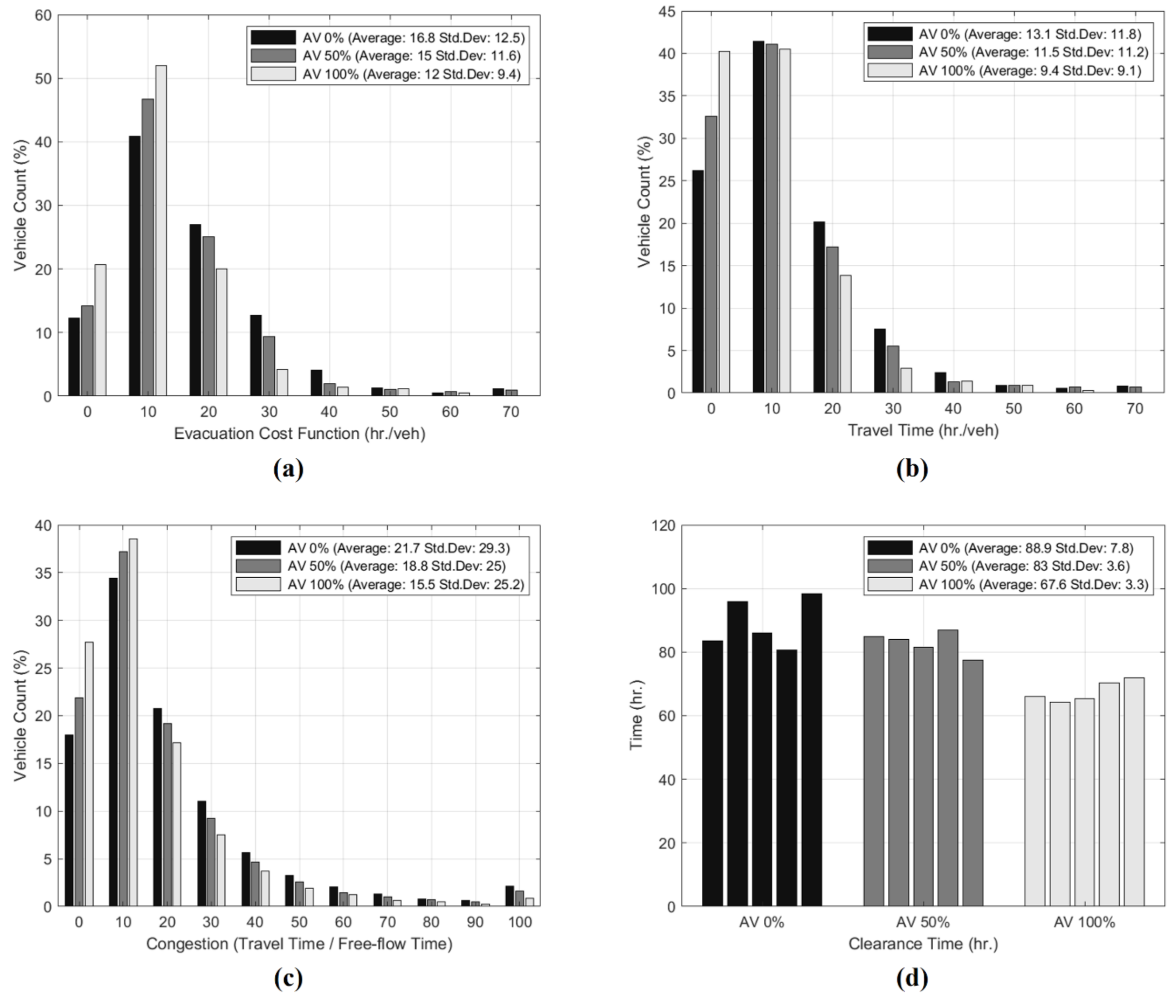

Figure 6. Evacuation Performance by AV Scenarios

Evacuation Time Scenario Analysis

The evacuation time scenario analysis evaluates the impact of different departure time schedules and evacuation time spans using the AV 0% scenario. The second column of Table 4 analyzes the impact of departure time schedule while fixing the evacuation time span to the optimal value (23.3 hr.). The panic departure time schedule demonstrates a panic case of everyone departing at once during the first interval regardless of the disaster. Compared to the optimal scenario (first column), the network clearance time is shorter (-4%), but all other estimates are higher (e.g., +20% travel time and +25% congestion). When residents are panicked and depart as early as possible, the clearance time may be shorter due to the earlier departure times, but the excessive congestion in the network results in higher evacuation cost and longer travel times.

Another evacuation time scenario analysis is performed by changing the evacuation time span while departure time schedule is fixed to the optimal value. According to the third column of Table 4, with a shorter evacuation time span, the result is similar to the panic case. The evacuees will be departing earlier than the optimal case, resulting in shorter clearance time (-5%), but the evacuees will experience longer travel time (+10%) and more congestion (+15%).

On the other hand, with a longer evacuation time span as shown in the fourth column, the travel time and congestion will decrease since the evacuation will occur during a more dispersed time span. However, this scenario will experience longer clearance time (+6%), so that some evacuees may be faced with possible threats during the evacuation. Moreover, none of the scenarios have a smaller evacuation cost compared to the optimal combination of evacuation time span and departure time schedule. Therefore, it is essential to schedule the evacuation by considering the combination of evacuation time span and departure time schedules.

Table 4. Evacuation Time Scenario Analysis

AV 0%	Optimal Evacuation Time Span (23.3 hr.)		Optimal Departure Time Schedule (52, 8, 18, 8, 14)	
	Optimal Departure Time Schedule (52, 8, 18, 8, 14)	Panic Departure Time Schedule (100, 0, 0, 0, 0)	Shorter Evacuation Time Span (14 hr.)	Longer Evacuation Time Span (30 hr.)
Evacuation Cost Average per Veh.	16.8 hr./veh	21.1 (+25.6%)	17.4 (+3.57%)	17.3 (+2.98%)
Evacuation Cost Std. Dev. per Veh.	12.4 hr./veh	13.8 (+11.3%%)	12.3 (-0.8%)	13 (+4.8%)
Travel Time Average per Veh.	13.1 hr./veh	15.7 (+19.9%)	14.4 (+9.9%)	11.9 (-9.2%)
Travel Time Std. Dev. per Veh.	11.8hr./veh	12.5 (+5.9%)	12 (+1.7%)	11.5 (-2.5%)
Clearance Time	88.9 hr.	85.8 (-3.5%)	84.8 (-4.6%)	94 (+5.7%)
Congestion (Travel Time / Free-flow Time)	21.7	27 (+24.4%)	24.9 (+14.8%)	19.4 (-10.6%)

(Values in parentheses show percentage change compared to optimal case)

CONCLUSIONS

This paper develops an evacuation time scheduling algorithm for both departure time scheduling and evacuation time span. The evacuation is posed as a bi-level game, where the upper level problem organizes evacuation time scheduling, and the lower level performs transportation and flood simulations. The developed algorithm is applied to the Houston network with a realistic flood simulation demonstrating Hurricane Harvey in 2017. AV adoption is combined with the evacuation time scheduling algorithm to evaluate the impact of AVs on the evacuation. However, the developed model can be applied to any transportation network and any type of disaster as long as the network configuration and disaster data are provided.

It is shown that the departure time schedule and evacuation time span are not sensitive to the penetration rate of AVs. The evacuation schedule is more sensitive to the timeline of the flood. However, more AVs in the network results in a smaller evacuation cost, leading to a more desirable evacuation performance. This is due to the increased capacity obtained from the quicker reaction time and headway of AV fleets. The evacuees will experience around 30% less evacuation cost, shorter travel time, reduced congestion, and shorter network clearance time with the adoption of AVs. This benefit is also applied to the standard deviation of evacuation cost and travel time, so that evacuees can expect more reliable evacuation in AV scenarios.

According to a scenario analysis of various evacuation time schedules, evacuees' panic or shorter evacuation time span may lead to shorter clearance time but will result in higher evacuation cost and severe congestion compared to the optimal scenario. On the other hand, a longer evacuation time span may reduce congestion but will result in a longer network clearance time than the optimal scenario. Therefore, the combination of departure time scheduling and evacuation time span is essential in improving evacuation performance.

Nonetheless, the simulation results suggest that it will take 3 to 4 days, even with the AV adoption, to completely evacuate everyone in the Houston network. The evacuees will spend 10 to 13 hours traveling on roads without adequate protection from disasters, due to traffic congestion. This suggests that additional operational methods, including contraflow (Wolshon, 2001), prioritization or tolling (Lee & Kockelman, 2019), and dynamic ride-sharing (Fagnant & Kockelman, 2018), should be combined with AV adoption and evacuation time scheduling to reduce network congestion.

ACKNOWLEDGEMENTS

This work is supported in part by Planet Texas 2050, a research grand challenge initiative of The University of Texas at Austin, with editing and administrative support from Jade (Maizy) Jeong. The authors acknowledge the Texas Advanced Computing Center (TACC) at The University of Texas at Austin for providing high performance computing resources that have contributed to the research results reported within this paper. The authors confirm contribution to the paper as follows: study conception and design: Kara Kockelman; data collection: Jooyong Lee, Kara Kockelman; analysis and interpretation of results: Jooyong Lee, Kara Kockelman; draft manuscript preparation: Jooyong Lee. All authors reviewed the results and approved the final version of the manuscript.

REFERENCES

Abdelgawad, H., Abdulhai, B., & Wahba, M. (2010). Multiobjective optimization for multimodal evacuation. *Transportation Research Record*, 2196(1), 21-33.

Apivatanagul, P., Davidson, R. A., & Nozick, L. K. (2012). Bi-level optimization for risk-based regional hurricane evacuation planning. *Natural hazards*, 60(2), 567-588.

Blake, E. S., & Zelinsky, D. A. (2018). National Hurricane Center Tropical Cyclone Report - Hurricane Harvey (AL092017). Accessed on July 20, 2020 at: https://www.nhc.noaa.gov/data/tcr/AL092017_Harvey.pdf. In: National Hurricane Center.

Chien, S. I., & Korikanthimath, V. V. (2007). Analysis and modeling of simultaneous and staged emergency evacuations. *Journal of Transportation Engineering*, 133(3), 190-197.

Elder, K., Xirasagar, S., Miller, N., Bowen, S. A., Glover, S., & Piper, C. (2007). African Americans' decisions not to evacuate New Orleans before Hurricane Katrina: A qualitative study. *American Journal of Public Health*, 97(Supplement_1), S124-S129.

Fagnant, D. J., & Kockelman, K. M. (2018). Dynamic ride-sharing and fleet sizing for a system of shared autonomous vehicles in Austin, Texas. *Transportation*, 45(1), 143-158.

Federal Emergency Management Agency. (FEMA, 2018). FEMA - Harvey Flood Depths Grid, HydroShare. Accessed on July 2, 2020 at: https://doi.org/10.4211/hs.165e2c3e335d40949dbf501c97827837.

Federal Highway Administration. (FHA, 2017). National Household Travel Survey - Count of Household

Vehicles. Accessed on July 3, 2020 at: https://nhts.ornl.gov/. from U.S. Department of Transportation

Huang, S.-K., Lindell, M. K., & Prater, C. S. (2016). Who leaves and who stays? A review and statistical meta-analysis of hurricane evacuation studies. *Environment and Behavior*, 48(8), 991-1029.

Lee, J., & Kockelman, K. M. (2019). Development of Traffic-Based Congestion Pricing and Its Application to Automated Vehicles. *Transportation Research Record*, 2673(6), 536-547.

Levin, M. W., & Boyles, S. D. (2016). A multiclass cell transmission model for shared human and autonomous vehicle roads. *Transportation Research Part C: Emerging Technologies*, 62, 103-116.

Li, J., Ozbay, K., Bartin, B., Iyer, S., & Carnegie, J. A. (2013). Empirical evacuation response curve during hurricane irene in cape may county, new jersey. *Transportation Research Record*, 2376(1), 1-10.

Liu, X., & Lim, S. (2016). Integration of spatial analysis and an agent-based model into evacuation management for shelter assignment and routing. *Journal of Spatial Science*, 61(2), 283-298.

Lopez, P. A., Behrisch, M., Bieker-Walz, L., Erdmann, J., Flötteröd, Y.-P., Hilbrich, R., . . . WieBner, E. (2018). Microscopic traffic simulation using sumo. Paper presented at the 2018 21st International Conference on Intelligent Transportation Systems (ITSC).

Lämmel, G., & Klüpfel, H. (2012). Slower is faster: the influence of departure time distribution on the overall evacuation performance. Paper presented at the International Conference on Evacuation Modeling and Management.

Madireddy, M., Kumara, S., Medeiros, D., & Shankar, V. N. (2015). Leveraging social networks for efficient hurricane evacuation. *Transportation Research Part B: Methodological*, 77, 199-212.

Martín, Y., Li, Z., & Cutter, S. L. (2017). Leveraging Twitter to gauge evacuation compliance: Spatiotemporal analysis of Hurricane Matthew. *PLoS one*, 12(7), e0181701.

Morss, R. E., Demuth, J. L., Lazo, J. K., Dickinson, K., Lazrus, H., & Morrow, B. H. (2016). Understanding public hurricane evacuation decisions and responses to forecast and warning messages. *Weather and Forecasting*, 31(2), 395-417.

Pyakurel, U., Dhamala, T. N., & Dempe, S. (2017). Efficient continuous contraflow algorithms for evacuation planning problems. *Annals of Operations Research*, 254(1-2), 335-364.

Sadri, A. M., Ukkusuri, S. V., & Gladwin, H. (2017). Modeling joint evacuation decisions in social networks: The case of Hurricane Sandy. *Journal of Choice Modelling*, 25, 50-60.

Takabatake, T., Shibayama, T., Esteban, M., Ishii, H., & Hamano, G. (2017). Simulated tsunami evacuation behavior of local residents and visitors in Kamakura, Japan. *International Journal of Disaster Risk Reduction*, 23, 1-14.

Takagi, H., Li, S., de Leon, M., Esteban, M., Mikami, T., Matsumaru, R., . . . Nakamura, R. (2016). Storm surge and evacuation in urban areas during the peak of a storm. *Coastal Engineering*, 108, 1-9.

Tamminga, G., Tu, H., Daamen, W., & Hoogendoorn, S. (2011). Influence of departure time spans and corresponding network performance on evacuation time. *Transportation Research Record*, 2234(1), 89-96.

US Census Bureau. (2019). Quick Facts: Brazoria, Chambers, Fort Bent, Galveston, Harris, Liberty, Montgomery, and Waller County, TX-Population Estimates. Accessed on July 3, 2020 at: https://www.census.gov/quickfacts/fact/table/US/PST045219.

United States Geological Survey. (USGS, 2020). National Water Information System: Web Interface. Accessed on July 2, 2020 at: https://nwis.waterdata.usgs.gov/.

Wolshon, B. (2001). "One-way-out": contraflow freeway operation for hurricane evacuation. *Natural Hazards Review*, 2(3), 105-112.